Preventing presbycusis in mice with enhanced medial olivocochlear feedback

Luis E. Boero[a,b,1], Valeria C. Castagna[a,b,1], Gonzalo Terreros[c,d], Marcelo J. Moglie[b], Sebastián Silva[d,e,f], Juan C. Maass[d,e,f], Paul A. Fuchs[g], Paul H. Delano[d,h], Ana Belén Elgoyhen[a,b], and María Eugenia Gómez-Casati[a,2]

[a]Instituto de Farmacología, Facultad de Medicina, Universidad de Buenos Aires, 1121 Buenos Aires, Argentina; [b]Instituto de Investigaciones en Ingeniería Genética y Biología Molecular, Dr. Héctor N. Torres, Consejo Nacional de Investigaciones Científicas y Técnicas, 1428 Buenos Aires, Argentina; [c]Instituto de Ciencias de la Salud, Universidad de O'Higgins, 2841935 Rancagua, Chile; [d]Laboratory of Auditory Neurobiology, Auditory and Cognition Center, 8380453 Santiago, Chile; [e]Programa Interdisciplinario de Fisiología y Biofísica, Instituto de Ciencias Biomédicas, Universidad de Chile, 8380453 Santiago, Chile; [f]Departamento de Otorrinolaringología, Facultad de Medicina, Universidad de Chile, 8380453 Santiago, Chile; [g]The Center for Hearing and Balance, Otolaryngology-Head and Neck Surgery, Johns Hopkins University School of Medicine, Baltimore, MD 21205; and [h]Departamento de Neurociencia y Otorrinolaringología, Facultad de Medicina, Universidad de Chile, 8380453 Santiago, Chile

Edited by Dan H. Sanes, New York University, New York, NY, and accepted by Editorial Board Member J. Anthony Movshon April 1, 2020 (received for review January 19, 2020)

"Growing old" is the most common cause of hearing loss. Age-related hearing loss (ARHL) (presbycusis) first affects the ability to understand speech in background noise, even when auditory thresholds in quiet are normal. It has been suggested that cochlear denervation ("synaptopathy") is an early contributor to age-related auditory decline. In the present work, we characterized age-related cochlear synaptic degeneration and hair cell loss in mice with enhanced α9α10 cholinergic nicotinic receptors gating kinetics ("gain of function" nAChRs). These mediate inhibitory olivocochlear feedback through the activation of associated calcium-gated potassium channels. Cochlear function was assessed via distortion product otoacoustic emissions and auditory brainstem responses. Cochlear structure was characterized in immunolabeled organ of Corti whole mounts using confocal microscopy to quantify hair cells, auditory neurons, presynaptic ribbons, and postsynaptic glutamate receptors. Aged wild-type mice had elevated acoustic thresholds and synaptic loss. Afferent synapses were lost from inner hair cells throughout the aged cochlea, together with some loss of outer hair cells. In contrast, cochlear structure and function were preserved in aged mice with gain-of-function nAChRs that provide enhanced olivocochlear inhibition, suggesting that efferent feedback is important for long-term maintenance of inner ear function. Our work provides evidence that olivocochlear-mediated resistance to presbycusis-ARHL occurs via the α9α10 nAChR complexes on outer hair cells. Thus, enhancement of the medial olivocochlear system could be a viable strategy to prevent age-related hearing loss.

hearing loss | aging | cochlear synaptopathy | medial olivocochlear system

Functional deterioration of the nervous system is an important feature of aging. Age-related hearing loss (ARHL) (presbycusis) commonly afflicts the elderly, with almost one in three adults over age 65 experiencing some degree of hearing loss (1, 2). Population-based observational studies have shown that hearing impairment is strongly related to accelerated cognitive decline and dementia risk in older adults (3–5). Indeed, hearing loss is now known to be the largest modifiable risk factor for developing dementia, exceeding that of smoking, high blood pressure, lack of exercise, and social isolation (6). Given the high prevalence and its strong association with dementia, presbycusis is a compelling problem for society, resulting in a high economic impact (7). There is a general consensus that ARHL is a multifactorial progressive disease produced by different factors, such as continuous exposure to high levels of noise, ototoxic compounds, trauma, history of otologic disease, vascular insults, metabolic changes, diet, and immune system, that are superimposed upon an intrinsic, genetically controlled aging process (8). Although the potential mechanisms underlying ARHL have not been established, the age-related decline in acuity is mostly attributed to damage to peripheral sensory and neural elements, as well as changes occurring along the central auditory pathway (9–11). Peripheral degeneration involves the degeneration of the stria vascularis, sensory hair cells, spiral ganglion neurons, and fibrocytes. ARHL usually begins at the higher frequencies, degrading speech intelligibility in background noise and causing impaired localization of sound sources (2).

It has recently been shown that synaptic connections between hair cells and auditory nerve fibers are lost well before hair cells are damaged or auditory thresholds elevated in aged cochleae (12–14). This synaptic degeneration can progressively silence large numbers of cochlear afferent neurons but does not impact auditory threshold tests until the neuronal loss is almost complete (15, 16). Such cochlear synaptopathy could underlie poor speech discrimination in noisy environments (17, 18) and may contribute to the generation of tinnitus, hyperacusis, and associated perceptual abnormalities (19–24).

Olivocochlear efferent neurons project from the superior olivary complex to the cochlea. Medial olivocochlear (MOC) neurons innervate outer hair cells (OHCs) to form a negative feedback, gain-control system for cochlear amplification of sounds (25–27). Activation of the MOC pathway, either by sound

Significance

Age-related hearing loss is the most common cause of hearing loss. Here, we show that medial olivocochlear feedback mediates resistance to age-related hearing loss—presbycusis—and that this occurs via the α9α10 cholinergic nicotinic receptor complexes on outer hair cells. These findings are particularly promising because they provide a proof of principle supporting the enhancement of the medial olivocochlear system as a viable approach for prevention or treatment of age-related hearing loss. Therefore, it opens the way to the design of novel positive modulators of α9α10 nAChR receptors for clinical use in the prevention of both noise and age-related hearing loss.

Author contributions: L.E.B., V.C.C., G.T., P.A.F., P.H.D., A.B.E., and M.E.G.-C. designed research; L.E.B., V.C.C., G.T., S.S., and M.E.G.-C. performed research; A.B.E. and M.E.G.-C. contributed new reagents/analytic tools; L.E.B., V.C.C., G.T., M.J.M., J.C.M., and M.E.G.-C. analyzed data; and M.E.G.-C. wrote the paper.

The authors declare no competing interest.

This article is a PNAS Direct Submission. D.H.S. is a guest editor invited by the Editorial Board.

[1]L.E.B and V.C.C contributed equally to this work.

[2]To whom correspondence may be addressed. Email: megomezcasati@gmail.com.

This article contains supporting information online at https://www.pnas.org/lookup/suppl/doi:10.1073/pnas.2000760117/-/DCSupplemental.

First published May 11, 2020.

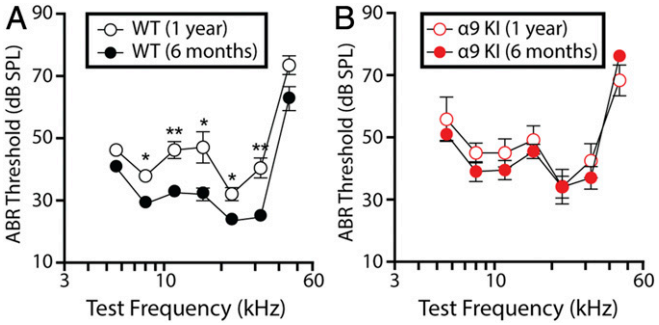

Fig. 1. Auditory function in young and aged WT and α9KI mice. (*A*) ABR thresholds for WT mice at 6 mo (n = 10) and 1 y of age (n = 6). (*B*) ABR thresholds for α9KI mice at 6 mo (n = 10) and 1 y of age (n = 6). At 1 y of age, cochlear thresholds were elevated in WT but not in α9KI mice. Group means ± SEM are shown. Asterisks represent the statistical significance (Friedman test, *P < 0.05 and **P < 0.01).

or by shock trains delivered to the bundle at the level of the IVth ventricle, reduces cochlear sensitivity through the action of the neurotransmitter acetylcholine (ACh) on α9α10 nAChRs, present at the base of OHCs, and coupled to calcium-dependent SK2 potassium channels (27–29). Although significant advancement has been made in defining the cellular mechanisms of hair cell inhibition (30–34), the functional role(s) of this sound-evoked feedback system remains open to discussion. Animal studies have shown that the MOC system may mediate selective attention by suppressing sound responses when performing a visual task (35, 36), improve discrimination of complex stimuli in a noisy background (37, 38), and adjust afferent signals from the two ears to allow the central processor to maintain accuracy in sound localization after unilateral conductive hearing loss (39). In addition, several reports have revealed that the MOC system has an important role in the protection from noise-induced hearing loss (40–45). Other studies have demonstrated that age-related changes in the MOC system play a role in the progression of presbycusis in mammals (46–50). A more recent study used olivocochlear bundle lesion to suggest that efferent-mediated protection helps to maintain normal synaptic function in the aged ear (12).

Our work explores the extent of presbycusis in mice with genetically enhanced MOC feedback: i.e., an α9 nAChR point mutation that leads to enhanced responses to ACh released by MOC fibers (α9 knockin [α9KI] mice) (45). We precluded exposure to high levels of sounds as a confounding factor in the aging process by maintaining mice in a sound-controlled room. We found that mutant mice were protected from the loss of acoustic sensitivity and the decreased auditory brainstem response amplitude that occurred in year-old wild-type (WT) mice. Moreover, the degree of cochlear synaptopathy and hair cell loss were reduced in aged α9KI compared to WT mice. The present results show that strengthening MOC feedback by enhancement of α9α10 nAChR activity can slow cochlear aging. Thus, drugs acting as positive modulators of α9α10 nAChR-mediated responses could have a therapeutic use in preventing or delaying presbycusis.

Results

Auditory Function in Aged Mice with Enhanced Efferent Inhibition. Auditory brainstem responses (ABRs), the sound-evoked potentials produced by neuronal circuits in the ascending auditory pathway, were recorded to evaluate cochlear function at two different time points: 6 mo (young) and 1 y of age (aged) in mice with different levels of MOC function raised in a sound-controlled room in the animal facility. As shown in Fig. 1*A*, mean ABR thresholds were significantly elevated in aged WT mice at all frequencies, except for the highest (45.25 kHz) and lowest (5.6 kHz). Elevations ranged as follows: Friedman test, 29.5 ± 1.3–37.9 ± 1.0 dB sound pressure level (SPL) at 8 kHz ($\chi2$ = 7.3, degree of freedom [df] = 1, P = 0.01); 33.0 ± 1.4–46.3 ± 2.7 dB SPL at 11.33 kHz ($\chi2$ = 6.5, df = 1, P = 0.003); 32.5 ± 1.9–47.1 ± 5.0 dB SPL at 16 kHz ($\chi2$ = 7.5, df = 1, P = 0.02); 24.0 ± 1.2–32.1 ± 2.1 dB SPL at 22.65 kHz ($\chi2$ = 6.2, df = 1, P = 0.01); and 25.2 ± 1.4–40.4 ± 3.2 dB SPL at 32 kHz ($\chi2$ = 2.4, df = 1, P = 0.003). However, no differences in mean ABR thresholds were found between young and aged α9KI with enhanced MOC feedback (Friedman test, df = 1, P > 0.05 at all of the frequencies) (Fig. 1*B*). It is important to note that, at 6 mo, mean ABR thresholds were slightly elevated in α9KI compared to the same age WT mice at all of the frequencies (Fig. 1, compare filled red and black circles). Elevations ranged as follows: Friedman test, 41.0 ± 1.7–51.0 ± 2.0 dB SPL at 5.6 kHz ($\chi2$ = 3.8, df = 1, P = 0.012); 29.5 ± 1.3–39.0 ± 3.2 dB SPL at 8 kHz ($\chi2$ = 2.8, df = 1, P = 0.013); 33.0 ± 1.4–39.5 ± 3.1 dB SPL at 11.33 kHz ($\chi2$ = 1.9, df = 1, P = 0.04); 32.5 ± 2.0–45.5 ± 2.3 dB SPL at 16 kHz ($\chi2$ = 4.3, df = 1, P = 0.001); 24.0 ± 1.2–34.0 ± 3.5 dB SPL at 22.65 kHz ($\chi2$ = 2.7, df = 1, P = 0.02); 25.2 ± 1.4–37.0 ± 3.6 dB SPL at 32 kHz ($\chi2$ = 3.1, df = 1, P = 0.02); and 63.0 ± 3.8–76.2 ± 1.3 dB SPL at 45.25 kHz ($\chi2$ = 3.3, df = 1, P = 0.004). The same ABR threshold elevations were reported previously both at 2 mo (45) and postnatal day 21 (P21) (43).

OHC function was assessed through distortion product otoacoustic emissions (DPOAEs) recorded from the external auditory canal (51). In the normal cochlea stimulated simultaneously by two close pure tone frequencies, distortions are created by nonlinearities in OHC transduction. These distortion products are amplified by OHC electromotility, causing motion at the distortion frequencies that propagates to the middle ear and can be detected by a microphone in the external ear canal (51, 52). As shown in Fig. 2*A*, DPOAE thresholds were elevated at all of the frequencies at 1 y of age in WT ears, with normal MOC feedback, except at the highest frequency tested (45.25 kHz). Elevations ranged as follows: Friedman test, 63.0 ± 5.2–80.0 ± 2.2 dB SPL at 5.6 kHz ($\chi2$ = 3, df = 1, P = 0.008); 47.5 ± 6.3–61.7 ± 4.0 dB SPL at 8 kHz ($\chi2$ = 3.3, df = 1, P = 0.02); 37.5 ± 4.4–46.7 ± 1.7 dB SPL at 11.33 kHz ($\chi2$ = 4.5, df = 1, P = 0.01); 28.5 ± 2.0–57.5 ± 3.3 dB SPL at 16 kHz ($\chi2$ = 5.8, df = 1, P < 0.001); 29.0 ± 1.2–47.5 ± 1.1 dB SPL at 22.65 kHz ($\chi2$ = 10.1, df = 1, P = 0.001); and 30.0 ± 2.9–40.0 ± 1.3 dB SPL at 32 kHz ($\chi2$ = 6.5, df = 1, P = 0.017). In contrast, DPOAE thresholds were identical in 6-mo-old and 1-y-old α9KI mice (Friedman test, df = 1, P > 0.05 at all of the frequencies), indicating that OHC function is not degraded in

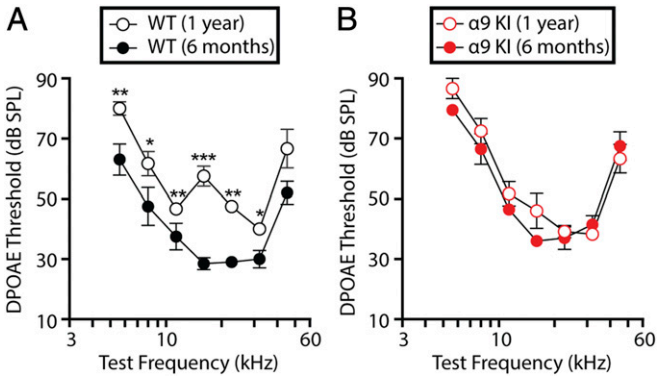

Fig. 2. Evaluation of OHC functional integrity in young and aged WT and α9KI mice. (*A*) DPOAE thresholds for WT mice at 6 mo (n = 10) and 1 y of age (n = 6). (*B*) DPOAE thresholds for α9KI mice at 6 mo (n = 10) and 1 y of age (n = 6). DPOAE thresholds showed a significant increase at 1 y of age in WT but not in α9KI mice. Group means ± SEM are shown. Asterisks represent the statistical significance (Friedman test *P < 0.05, **P < 0.01, and ***P < 0.001).

aged mice with enhanced MOC inhibition. As observed for ABR thresholds, mean DPOAE thresholds were elevated in α9KI at 6 mo compared to the same age WT mice at all frequencies (Fig. 2, compare filled red and black circles). Elevations ranged as follows: Friedman test, 63.0 ± 5.2–79.5 ± 0.5 dB SPL at 5.6 kHz ($\chi2 = 3.17$, df = 1, $P = 0.005$); 47.5 ± 6.3–66.5 ± 5.1 dB SPL at 8 kHz ($\chi2 = 2.36$, df = 1, $P = 0.03$); 37.5 ± 4.4–46.5 ± 1.8 dB SPL at 11.33 kHz ($\chi2 = 4.1$, df = 1, $P = 0.02$); 28.5 ± 2.0–36.0 ± 1.8 dB SPL at 16 kHz ($\chi2 = 2.8$, df = 1, $P = 0.03$); 29.0 ± 1.2–37.0 ± 3.7 dB SPL at 22.65 kHz ($\chi2 = 3.5$, df = 1, $P = 0.02$); 30.0 ± 2.9–41.5 ± 3.0 dB SPL at 32 kHz ($\chi2 = 2.2$, df = 1, $P = 0.04$); and 52.0 ± 3.8–67.5 ± 4.7 dB SPL at 45.25 kHz ($\chi2 = 3.1$, df = 1, $P = 0.03$). Similarly, the same DPOAE threshold elevations were observed at early stages (P21 and 2 mo old) (43, 45). Since MOC efferents are sensitively driven by sound (53, 54), the increased cochlear thresholds (both in ABRs and DPOAEs) observed in young mutant mice might reflect enhanced synaptic inhibition via mutant α9-containing channels. Indeed, this seems to be the case since elevated acoustic thresholds of α9KI mice are normalized by injection of the α9α10 nAChR antagonist strychnine (45), consistent with stronger feedback inhibition.

ABR waveforms involve a succession of peaks within the first ~7 ms after sound stimulus onset (peaks 1 to 5). As shown in Fig. 3*A*, comparison of ABR waveforms in WT versus α9KI mice (at 32 kHz, 80 dB SPL) revealed that age-related reductions in peak 1 amplitudes were greater than those in the later peaks, which arise from higher centers in the auditory brainstem. We therefore analyzed suprathreshold ABR peak 1 amplitudes at different frequencies. These represent the summed sound-evoked spike activity at the first synapse between inner hair cells (IHCs) and afferent nerve fibers (55). Normal cochleae display linear rises in peak 1 amplitudes in response to increasing sound stimulus whereas neuropathic cochleae do not (56). As shown in Fig. 3*B*, at 6 mo, there was no alteration in the mean ABR peak 1 suprathreshold amplitudes in α9KI compared to WT mice (Mann–Whitney *U* test, df = 1, $P > 0.05$ at all of the frequencies tested). However, at 1 y, there was a reduction in amplitudes in WT ears that was significant at high frequencies when compared to mutant mice (Mann–Whitney *U* test, $U = 2.1$, df = 1, $P = 0.02$ at 22.65 kHz; $U = 2.4$, df = 1, $P = 0.04$ at 32 kHz; and $U = 2.6$, df = 1, $P = 0.02$ at 45.25 kHz) (Fig. 3*C*). In WT mice, age-related decreases in suprathreshold response amplitudes appeared at all of the frequencies but were significant only at high frequencies (Friedman test, $\chi2 = 4.6$, df = 1, $P = 0.04$ at 22.65 kHz; $\chi2 = 3.9$, df = 1, $P = 0.01$ at 32 kHz; and $\chi2 = 4.3$, df = 1, $P < 0.001$ at 45.25 kHz), indicative of age-related changes in cochlear neural function (Fig. 3 *B* and *C*, compare filled and unfilled black circles). In contrast, there were no age-related changes in ABR waveforms of α9KI mice (Friedman test, df = 1, $P > 0.05$ at all of the frequencies tested) (Fig. 3 *B* and *C*, compare filled and unfilled red dots), suggesting that enhanced α9α10 nAChR activity might prevent the degeneration of afferent synapses. Altogether, these results show that the degree of age-related functional inner ear impairment depends on the level of α9α10 nAChR activity.

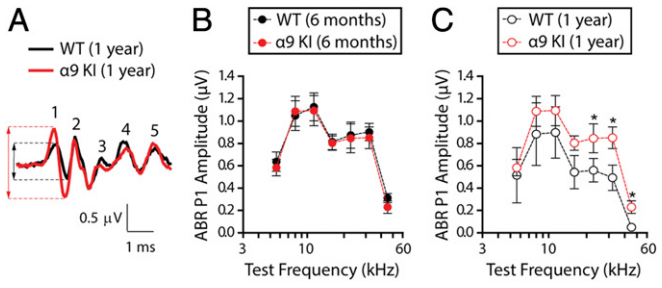

Fig. 3. Suprathreshold response amplitude for ABR peak 1 in young and aged WT and α9KI mice. (*A*) Representative ABR waveforms (32 kHz, 80 dB SPL) from WT (black) and α9KI (red) mice at 1 y of age showed a large reduction in wave 1 amplitudes. Dashed lines mark peak 1 amplitude from aged WT (black) and α9KI (red) mice. (*B*) ABR peak 1 amplitudes at 80 dB SPL in WT ($n = 10$) and α9KI ($n = 10$) mice at 6 mo of age at different test frequencies. (*C*) ABR peak 1 amplitudes at 80 dB SPL in WT ($n = 6$) and α9KI ($n = 6$) mice at 1 y of age. Aged WT ears displayed a significant reduction in peak 1 amplitudes at high frequencies. Group means ± SEM. Asterisks represent the statistical significance (Mann–Whitney *U* test, $^*P < 0.05$).

Age-Related Cochlear Synaptopathy and OHC Degeneration. After physiological testing, cochleae were harvested and fixed for histological analysis at 6 mo and 1 y. To analyze the synapses between IHCs and auditory nerve fibers, organ of Corti whole mounts were immunostained with antibodies against CtBP2-Ribeye, a critical protein present at the presynaptic ribbon (57) and GluA2 AMPA-type glutamate receptors (AMPARs), which are expressed at the postsynaptic afferent terminal (42, 58, 59). IHC-afferent synapses were identified by colocalization of a pair of CtBP2/GluA2 puncta at the base of the IHC (59) (Fig. 4*A*). The number of colocalized synaptic puncta per IHC was not altered in α9KI compared to WT mice at 6 mo of age (Fig. 4 *A* and *B*). Quantitative analysis shows that, at the midbasal cochlear turn, there was no difference in the total number of synaptic puncta per IHC in young WT compared to mutant mice (Mann–Whitney *U* test, df = 1, $P > 0.05$) (Fig. 4*B*). Previous studies have described complementary gradients of CtBP2/GluA2 at the cochlear-nerve/IHC synapses whereby synapses from the modiolar face and/or basal pole of the IHC have larger ribbons and smaller AMPAR patches than synapses located in the opposite (pillar face) region of the cell (59). We computed the fluorescence volume information for both synaptic components by plotting the GluA2 volumes against CtBP2 volumes (i.e., colocalized ribbons and AMPAR patches) from confocal z-stacks comprising ~10 IHCs from the entire cochlear turns using the analysis previously described (60, 61). As shown in Fig. 4*C*, the inverse correlation between the sizes of ribbon and AMPAR components was quite prominent and did not differ between young WT and α9KI mice (F test, F = 1.58, df = 1, $P = 0.21$). This indicates that there was no impact on the spatial organization of afferent synapses at 6 mo in the mutants. Notably, at 1 y of age, the numbers of pre, post, and colocalized synaptic markers per IHC were higher in mice with enhanced MOC function at three different cochlear locations: apical, medial, and basal (Mann–Whitney *U* test; apical: $U = 50.5$, df = 1, $P < 0.001$; medial: $U = 43.2$, df = 1, $P < 0.0001$; and basal: $U = 48$, df = 1, $P < 0.0001$) (Fig. 5 *A*–*D*). Putative ribbon synapse counts, defined as juxtaposed CtBP2- and GluA2-positive puncta were ~20% fewer at the apical cochlear end in aged WT compared to α9KI mice (Fig. 5*D*). This difference was more pronounced in the medial and high (basal-end) frequency regions with 44% and 39% fewer synapses (Fig. 5*D*). As seen from the representative confocal pictures from immunostained organ of Corti, aged WT mice had fewer synapses with large ribbons and small AMPAR patches, known to correspond to the modiolar/basal zone of the IHCs (Fig. 5*A*) (59). After rotating the z-stack image to view the projection of one IHC as a cross-section through the cochlear epithelium (i.e., the *yz* plane) (Fig. 5*B*), the specific reduction of fibers with bigger synaptic ribbons in aged WT mice is even clearer. Analysis of double-stained cochlear epithelia (using 4× digital zoom) revealed that presynaptic and postsynaptic elements in aged WT ears tend to have large AMPAR patches and small ribbons while aged α9KI mice presented both types: large AMPAR patches paired with small ribbons and small AMPAR with large ribbons (Fig. 5*C*). Synaptic volume analysis showed that, in aged WT mice, the prevalence of large CtBP2- paired with small GluA2-positive puncta was

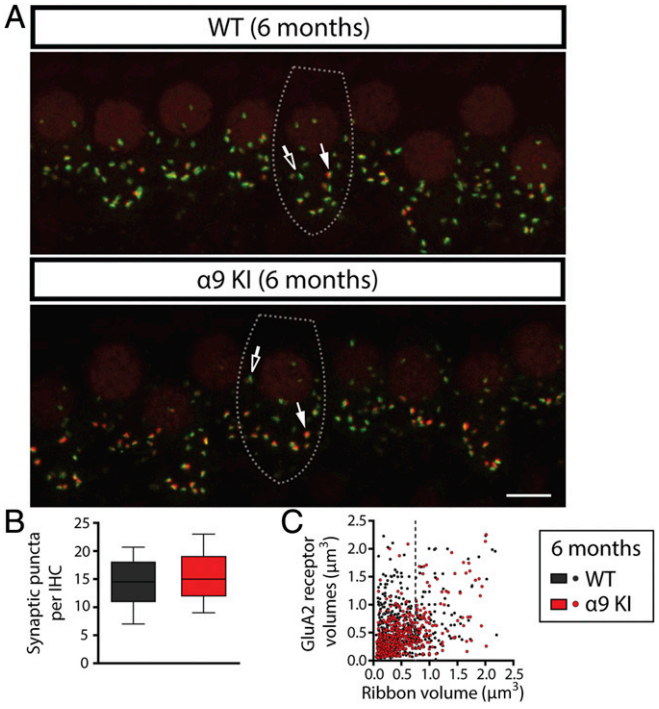

Fig. 4. Analysis of IHC ribbon synapses in young WT and α9KI mice. (*A*) Representative confocal images of IHC synapses from the middle region of cochleae immunolabeled for presynaptic ribbons (CtBP2-red) and postsynaptic receptor patches (GluA2-green) from WT (*Top*) and α9KI (*Bottom*) mice at 6 mo of age. (Scale bar: 10 μm.) The dashed lines show the approximate outline of one IHC. Afferent synapses in IHC show opposite gradients in the size of the presynaptic and postsynaptic elements: synapses with large ribbons and small AMPAR patches (filled arrows) and those with large AMPAR patches and small ribbons (open arrows). CtBP2 antibody also weakly stains IHC nuclei. (*B*) Quantitative data obtained from young WT and α9KI mice at the midbasal cochlear turn. For each IHC, the number of putative ribbon synapses was analyzed: i.e., colocalized CtBP2 and GluA2 puncta (WT = 185 IHCs from 10 animals; α9KI = 306 IHCs from 10 animals). Horizontal lines inside the box plots represent the median, and whiskers correspond to percentiles 10 to 90. Comparisons were made by a Mann–Whitney *U* test. (*C*) Scatter plots comparing the volumes of fluorescence staining for ribbons (CtBP2 volume, *x* axis) and receptors (GluA2 volume, *y* axis) for each of the synaptic pairs from young WT (517 synaptic pairs from five animals, slope = 0.41 ± 0.03) and α9KI tissues (508 synaptic pairs from five animals, slope = 0.49 ± 0.05) spanning the whole region of the cochlea. Comparisons were made by F test.

reduced, and small to medium-sized ribbons were prevalent (in Fig. 5*E*, the dashed line at a ribbon volume of 0.75 μm^3 illustrates this specific reduction in aged WT compared to aged α9KI mice). When aged WT and α9KI datasets were compared statistically using linear regression analysis, a significant difference was seen (F test, F = 13.29, df = 1, $P = 0.001$). The loss of synapses containing large ribbon patches in aged WT ears (Fig. 5*E*) is concurrent with the observed reduction in synaptic counts per IHC (Fig. 5*D*) and might be indicative of a selective loss of modiolar/basal fibers during aging. It is important to note that, as already shown (16, 62), maximum confocal projections at the medial cochlear region in aged WT mice showed a 30% reduction in synaptic counts compared to young WT ears (Mann–Whitney *U* test, $U = 16.85$, df = 1, $P < 0.0001$) (Figs. 4*B* and 5*D*), suggesting that, at 1 y of age, there is a substantial deafferentation of cochlear synapses. Likewise, as shown in Fig. 5*F*, volume distribution statistical analyses derived from young and aged WT datasets were substantially different from one another (F test, F = 19.10, df = 1, $P = 0.001$), indicating synaptic component size changes during aging (in Fig. 5*F*, see the specific reduction of synapses with large ribbons and small AMPAR patches after the dashed line at a ribbon volume of 0.75 μm^3 in aged WT). In contrast, no difference in synaptic counts in the medial cochlear region was observed in young and aged α9KI mice with enhanced MOC function (Mann–Whitney *U* test, df = 1, $P > 0.05$) (Figs. 4*B* and 5*D*). Similarly, no statistical difference was found in the scatter plots comparing the volumes of fluorescence staining for ribbons and AMPAR patches for each of the synaptic pairs in young and aged α9KI mice (F test, F = 3.39, df = 1, $P = 0.0657$) (Fig. 5*G*), suggesting that the enhanced strength of the olivocochlear reflex restrains cochlear synaptopathy.

To assess all cochlear nerve terminals and quantify any loss of hair cells in aged WT and α9KI mice, we used antineurofilament immunostaining to reveal all unmyelinated nerve fibers in the sensory epithelium combined with a fluorescent nuclear stain (blue channel: Draq5) (Fig. 6). We measured the density and thickness of nerve fibers across the cochlear epithelium by segregating the analysis considering the IHC and OHC areas of the organ of Corti. There was no overall significant difference in the density or thickness of neurofilament-positive elements between WT and α9KI mice at 1 y in any region evaluated (Fig. 6 *A*–*C*) (Mann–Whitney *U* test, df = 1, $P > 0.05$ at all of the cochlear regions). Moreover, no differences were observed in the fibers spiraling under the IHCs (Fig. 6*A*, unfilled arrows and Fig. 6*C*), which correspond to lateral olivocochlear fibers in the inner spiral bundle targeting cochlear nerve dendrites (56, 63). In addition, there was no alteration in the terminals crossing the tunnel of Corti (pillar cells' [PCs] region), which are mostly MOC fibers projecting to OHCs (Fig. 6*A*, thick fibers, filled arrows and Fig. 6*B*) and type II afferent neurons. Notably, in aged WT, loss of OHCs compared to α9KI ears was evident and significant at the apical and basal cochlear regions. There was a 5.1% and 6.3% of OHCs loss at the apical and basal end in aged WT mice, respectively (Mann–Whitney *U* test, $U = 7$, df = 1, $P = 0.007$ at the apical and $U = 9.5$, df = 1, $P = 0.004$ at the basal cochlear region) (Fig. 6*D*). In contrast, there was almost no OHC loss in those with enhanced MOC reflex (OHC loss in α9KI mice was less than 1.8% at all of the cochlear regions; Mann–Whitney *U* test, df = 1, $P > 0.05$). This result strongly suggests that the enhanced strength of the MOC system provides a protective effect against OHC damage.

Discussion

The design of effective therapeutics to prevent ARHL requires an understanding of the functionally important structural changes that underlie presbycusis. The present work shows that enhancement of the MOC system slows the progression of ARHL. Indeed, in contrast to WT, genetically modified mice carrying a "gain of function" point mutation in the α9 nAChR subunit exhibited neither cochlear synaptopathy nor OHC death during aging. In addition, different to WT, aged α9KI presented no reduction of suprathreshold ABR peak 1 amplitudes compared to 6-mo-old mice. Moreover, α9KI mice exhibited no ABR or DPOAE threshold elevations at 1 y of age, compared to those measured at 6 mo, indicating hearing preservation. The present findings are particularly promising because this protective effect is due to the "natural" activation of a modified efferent reflex by sound (53, 54). Thus, one can propose that the enhanced gating of modified α9 nAChRs increases the "gain" of the efferent acoustic reflex so that the protective effect rises more steeply as a function of sound level.

The mechanisms underlying ARHL–presbycusis are not well-understood. There is a general agreement that it is the consequence of several types of physiological degeneration plus the accumulated effects of noise exposure, as well as genetic susceptibility. The high level of noise exposure in modern industrialized societies makes acquired auditory stress a particularly significant

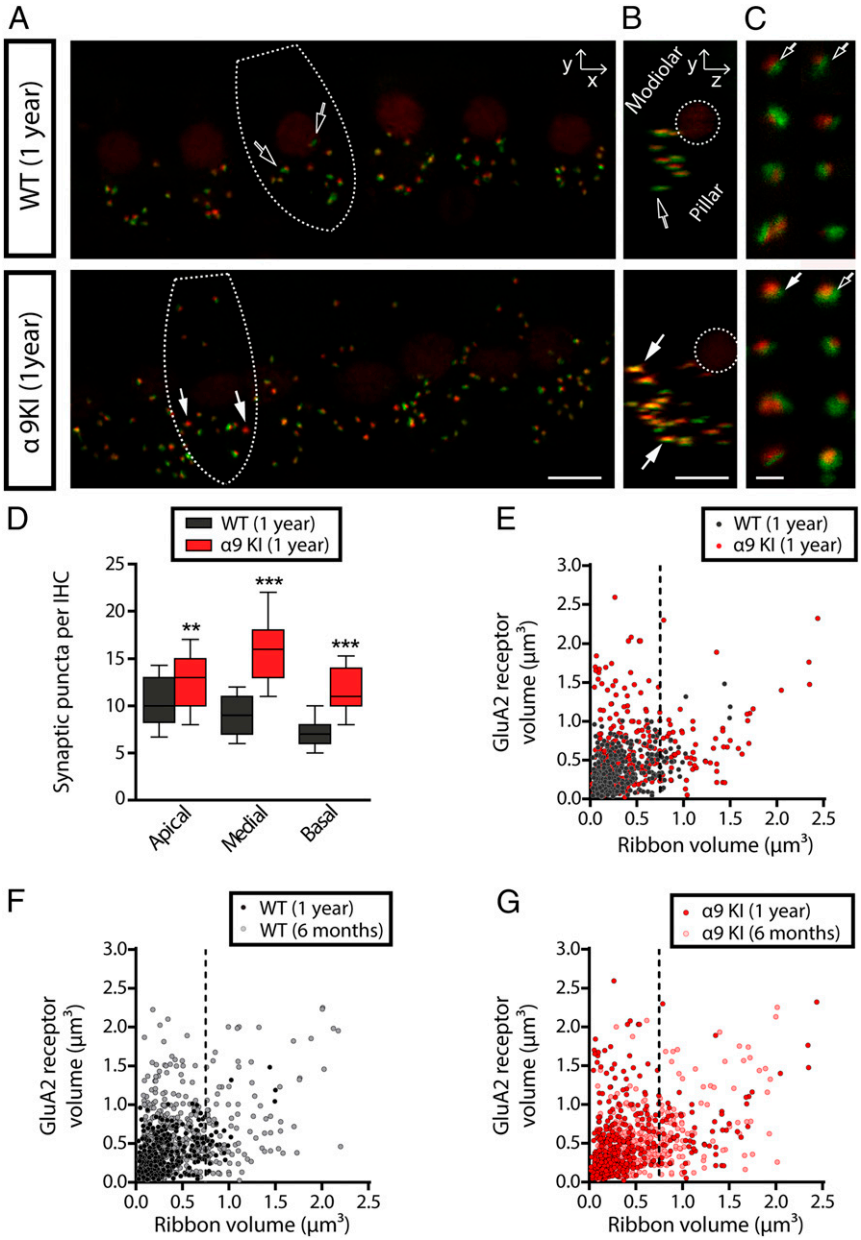

Fig. 5. Analysis of IHC ribbon synapses in aged WT and α9KI mice. (*A*) Representative confocal images in the xy projection of IHCs' synapses from the medial region of cochleae immunolabeled for presynaptic ribbons (CtBP2-red) and postsynaptic receptor patches (GluA2-green) from WT (*Top*) and α9KI (*Bottom*) mice at 1 y of age. (Scale bar: 10 μm.) The dashed lines show the approximate outline of one IHC. (*B*) Cochlear whole mount *yz* projection of one IHC. In WT mice, the largest AMPAR labels are on the pillar side, with fewer synapses on the modiolar/basal pole side of the IHC (scale bar: 10 μm). The dashed lines show the outline of the nucleus of one IHC. (*C*) Shown are 4× zoom images of afferent synapses from aged WT (*Top*) and α9KI (*Bottom*) mice. WT ears showed mainly a population of ribbon synapses with bigger AMPAR patches while α9KI ears showed both populations of ribbon synapses. (Scale bar: 0.5 μm.) Filled arrows indicate synapses with large ribbons and small AMPAR patches while unfilled ones show synapses with the smallest ribbons and largest AMPAR patches (*A*–*C*). (*D*) Quantitative data obtained from aged WT and α9KI mice. For each IHC, the number of putative ribbon synapses was analyzed: i.e., colocalized CtBP2 and GluA2 puncta (WT: 76 IHCs at the apical, 103 IHCs at the medial, and 102 IHCs at the basal region from 10 animals; α9KI: 208 IHCs at the apical, 108 IHCs at the medial, and 116 IHCs at the basal region from 10 animals). Horizontal lines inside the box plots represent the median, and whiskers correspond to percentiles 10 to 90. Asterisks represent the statistical significance (Mann–Whitney *U* test, $^{**}P < 0.01$ and $^{***}P < 0.001$). (*E*) Scatter plots comparing the volumes of fluorescence staining for ribbons (CtBP2 volume, *x* axis) and AMPAR (GluA2 volume, *y* axis) for each of the synaptic pairs from aged WT (412 synaptic pairs from four animals, slope = 0.23 ± 0.05) and α9KI tissues (553 synaptic pairs from five animals, slope = 0.42 ± 0.03) spanning the whole region of the cochlea. The dashed line (at ribbon volume of 0.75 μm^3) shows the reduction of synaptic pairs with bigger ribbons and smaller AMPAR patches in aged WT mice. Comparisons were made by F test. (*F*) Scatter plots comparing the volumes of fluorescence staining for ribbons and AMPAR for each of the synaptic pairs from young (517 synaptic pairs from four animals, slope = 0.49 ± 0.07) and aged (412 synaptic pairs from four animals, slope = 0.26 ± 0.07) WT mice. The dashed line (at ribbon volume of 0.75 μm^3) shows the reduction of synaptic pairs with bigger ribbons and smaller AMPAR patches in aged compared to young WT mice. Comparisons were made by F test. (*G*) Scatter plots comparing the volumes of fluorescence staining for ribbons and AMPAR for each of the synaptic pairs from young (508 synaptic pairs from four animals, slope = 0.37 ± 0.05) and aged (553 synaptic pairs from five animals, slope = 0.43 ± 0.07) α9KI tissues. The dashed line (at ribbon volume of 0.75 μm^3) shows that there is no alteration of synaptic pairs in aged compared to young α9KI mice. Comparisons were made by F test.

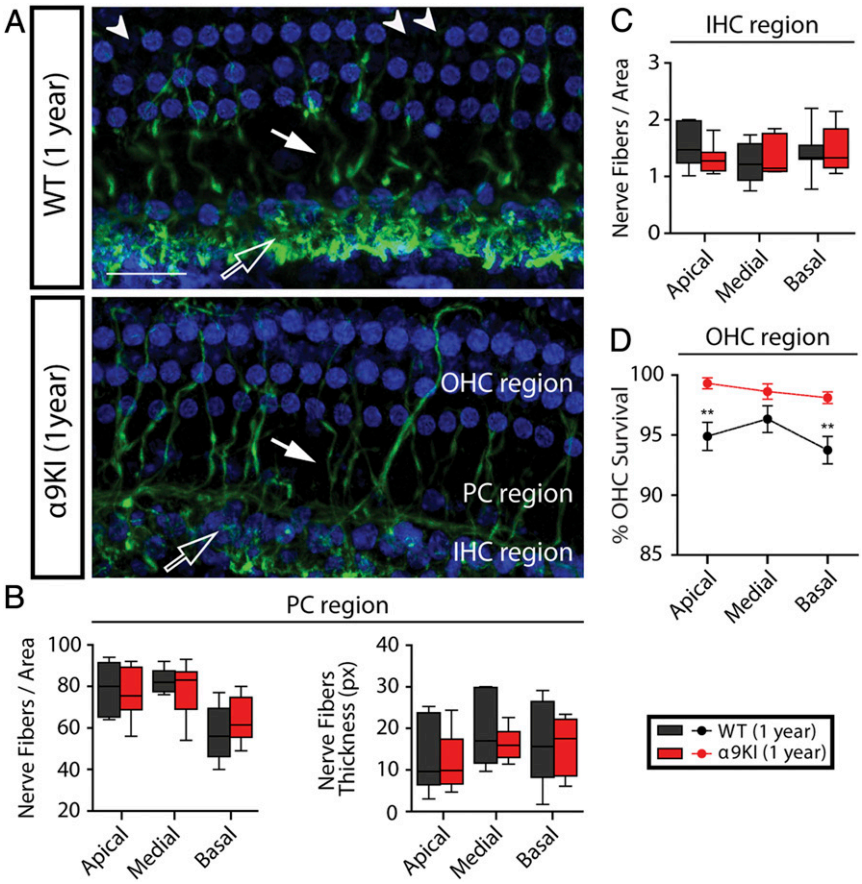

Fig. 6. OHCs and nerve fibers' quantification in aged WT and α9KI mice. (*A*) Representative confocal images of whole mounts organ of Corti immunolabeled for antineurofilament (green) and the nuclear dye Draq5 (blue) from WT (n = 10) and α9KI (n = 10) mice at 1 y of age (scale bar: 30 μm). Unfilled arrows indicate the thin fibers spiraling under the IHCs. MOC fibers projecting to OHCs and type II afferent neurons are indicated by filled arrows. Arrowheads point to lost OHCs. (*B*) Quantification of nerve fiber density and thickness at the PC region: nerve fiber density (*Left*) and thickness (*Right*) at the apical, medial, and basal portions of the cochlea. px, pixels. (*C*) Quantification of nerve fiber density at the IHCs' region in basal, medial, and apical portions of the cochlea. Horizontal lines inside the box plots (*B* and *C*) represent the median, and whiskers correspond to percentiles 10 to 90. (*D*) Mean OHC survival ± SEM is plotted as a function of cochlear location from WT and α9KI mice at 1 y of age. In aged WT, there was some loss of OHCs compared to α9KI ears that was significant at the apical and basal cochlear region. Asterisks represent the statistical significance (Mann–Whitney *U* test, $^{**}P < 0.01$).

factor, in addition to otological disease and intrinsic aging processes (8). Reduced cochlear sensitivity, degraded temporal resolution, and difficult hearing in background noise are commonly observed in the elderly with sensorineural hearing loss. Elevated cochlear threshold sensitivity is primarily peripheral in origin and related to hair cell damage or loss. Consistent with previous findings (16, 62, 64), the present work reports that 1-y-old WT mice exhibited elevated auditory thresholds, loss of cochlear synapses, and degeneration of OHCs. It is interesting to note that, in the present study, aged WT mice showed only a 5- to 20-dB SPL elevation in mean ABR thresholds at frequencies ranging from 5.6 to 45.25 kHz, compared to the 30- to 50-dB threshold shifts at all frequencies evidenced in the same strain of mice when exposed to damaging high noise levels (45). Since animals were raised in a sound-controlled room and not exposed to damaging loud sounds, one could conclude that the phenotype observed is only due to the intrinsic damaging process that occurs in aging ears and not to that resulting from the exposure to elevated sound pressure levels. This aging phenotype includes small ABR threshold shifts but an extent decrease of IHC synapses (with the concomitant decrease of suprathreshold ABR peak 1 amplitudes, reflecting reduced activation of auditory nerve fibers). Furthermore, at 1 y of age, there were also changes in DPOAE thresholds, together with a minimal, but significant, loss of OHCs. This finding could be the basis for the decline in acuity observed in old adults, particularly the lack of understanding of speech in noisy backgrounds at early stages of the aging process. Thus, it has been described that difficulty in understanding speech in noisy, reverberant environments occurs even when auditory thresholds in quiet are normal (65–69). The interruption in synaptic communication between sensory IHCs and subsets of cochlear nerve fibers is thought to contribute to these perceptual failures (24, 56). Indeed, cochlear synaptopathy has been identified as an early contributor to age-related auditory dysfunction (16). Since threshold shifts were very small in WT mice even at 1 y of age, but IHC synaptic loss was quite prominent, one could conclude that a routine auditory test does not fully assess the extent of damage to the hearing system produced during aging. This is in accordance with previous work (56) demonstrating that auditory thresholds are insensitive to widespread loss of IHC synapses after noise exposures causing only temporary threshold elevations.

The reduction of ABR peak 1 amplitudes in aged compared to young WT mice reflects a reduced activation of auditory nerve fibers. Furthermore, this reduction was matched by the loss of IHC-auditory nerve fiber synapses. The fact that the percentage of reduction in ABR peak 1 amplitudes at the medial and high (basal-end) frequency regions in aged WT was similar to the percentage of loss of ribbon synapses in the same regions supports the notion that this physiological parameter could be a useful measure of cochlear synaptopathy, as previously suggested (56). It has been described that age-dependent cochlear synaptic

degeneration in mice with normal MOC function grows constantly from weaning (4 wk) to death (~2.5 y), followed, after a few months, by a proportional loss of neuronal cell bodies (16). The degree of age-related cochlear neuropathy observed in WT mice at 1 y of age is consistent with this report. The loss of cochlear synapses in WT was not accompanied by a reduction of neurofilament-positive elements in these mice. Although this result could indicate a degeneration of synaptic terminals without a complete loss of fibers at 1 y of age (as previously described in ref. 56), the degeneration of terminals with some loss of afferent fibers that is not detected by the antineurofilament immunostaining technique used here cannot be precluded.

Noise-induced cochlear synaptopathy selectively impacts high threshold, low spontaneous rate ("low-SR") auditory nerve fibers (70). Studies of auditory neurons in aging gerbils also indicate a reduction in the proportion of low-SR fibers (71). In addition, aged C57BL/6 mice show a preferential loss of small afferent terminals on IHCs (14), thought to correspond to low-SR, high threshold fibers (72). In the present work, we found a reduction in the number of ribbon synapses in aged WT ears and that the remaining synapses have smaller ribbons and larger AMPAR patches. Since synapses with smaller ribbons and larger AMPAR are thought to be located in the pillar/apical zone of the IHC (59), the present results also indicate the selective loss of low-SR fibers in aging mice. However, we cannot disregard the possibility of relocation and/or dynamic changes in size of remaining ribbon synapses during aging. In fact, a recent work has shown noise-dependent alterations in resizing dynamics that occur in concert with changes in position of ribbon synapses (61). Given that low-SR fibers activate at high sound levels, selective loss of these fibers could explain why a 40% reduction of IHC-afferent fiber synapses (Fig. 5*B*) was associated with only 5- to 20-dB elevation of ABR thresholds (Fig. 1*A*) in aged WT mice. It has been proposed that high threshold, low-SR fibers are important for extending the dynamic range of hearing and contribute to hearing in a noisy environment (17, 18). Therefore, an age-related loss of low-SR fibers may be an important contributor to the decline of auditory performance in aging listeners, mostly related with speech-in-noise complications (73).

In contrast to that seen in WT mice, no modification in ABR thresholds or synaptic and OHC loss was observed in mice with enhanced MOC reflex. It is important to mention that genetically modified mice with enhanced MOC feedback already have a minimally elevated audiogram compared to WT mice. Thus, 6-mo-old α9KI mice displayed a 5- to 10-dB SPL ABR and DPOAE threshold elevation when compared with the age-matched WT mice. The same threshold difference has been described in previous reports in pubescent (43) and 2-mo-old mice (45). This increase in cochlear thresholds in mutant mice reflects an increased MOC efferent strength due to the enhanced synaptic inhibition via mutant α9-containing channels since thresholds in α9KI mice are normalized in the presence of the α9α10 nAChR antagonist strychnine (45). At 1 y of age, auditory thresholds in WT increase while those of α9KI mice remain unaffected compared to their respective controls. This lack of increase in ABR thresholds in the α9KI does not derive from a putative ceiling effect due to elevated (5- to 10-dB SPL) ABR thresholds at birth, but rather from a protective effect, since no loss of synapses and OHCs was observed. Moreover, it should be noted that up to 50-dB threshold elevations are observed in the FVB mice when exposed to loud sound pressure levels (45), indicating that 5 to 10 dB is not the maximal threshold elevation that can be attained in these mice under damaging conditions.

It has been proposed that the MOC reflex in adults controls the dynamic range of hearing (74), improves signal detection in background noise (38, 75, 76), is involved in selective attention (35, 36), and protects from acoustic injury (42, 43, 45, 77, 78). However, the impact of MOC feedback on the maintenance of cochlear nerve synapses in aged ears, in the absence of noise exposure, has not received much attention. It has been shown that IHCs' synapses are reduced in 45-wk-old mice after cochlear deefferentation achieved by surgical lesion of efferent pathways in the brainstem (12). However, efferent lesions in that study involved both lateral and medial olivocochlear subsystems. A properly placed midline cut at the floor of the IVth ventricle should remove the majority of MOC projections to both ears, while sparing most of the lateral olivocochlear fibers. Nonetheless, if the cut is slightly off midline, it will comprise axons of ipsilateral projecting medial and lateral cells (79). Our work provides evidence of MOC-mediated resistance to presbycusis–ARHL via α9α10 nAChR complexes on OHCs. Thus, increasing the magnitude of MOC effects, by increasing efferent potency through a gain-of-function α9α10 nAChR, renders mice more resistant to ARHL. Genetically enhanced α9α10 nAChRs maintain auditory sensitivity, preserving cochlear synapses and OHCs, suggesting that enhancement of the MOC system slows cochlear aging. The age-related loss of OHCs observed here in WT mice is quantitatively consistent with previous studies (16, 80, 81) and might account for much of the age-related threshold elevation in both ABR and DPOAEs in these mice. It is interesting to note that we observed a robust DPOAE threshold change together with a minimal OHC loss at 1 y of age in WT mice, suggesting OHCs dysfunction at this age. Thus, the elevation of DPOAE thresholds could be caused by OHC degeneration plus alterations in the functional properties of surviving OHCs, like alterations in electromotility by changes in the mechanotransduction and/or prestin properties during aging. It has been shown in humans that the longitudinal gradients of age-related OHC loss are complementary to those of the cochlear projections from the MOC system (82). Several reports have described that the density of MOC terminals on OHCs peaks at the middle region of the cochlea (83–85) and that there is an age-related decline during aging (46–50). Moreover, as the mouse ages, there are significant changes in the efficiency of the MOC suppression mechanism as elicited by contralateral narrowband stimuli, reinforcing the idea that age-related changes in the MOC or the operating points of OHCs might play a role in the progression of presbycusis in mammals (46–50). A similar midcochlear distribution of efferent terminals has recently been seen in human cochlea (86). Remarkably, our work shows greater age-related apical and basal loss of OHCs in WT compared to mice with enhanced MOC feedback, suggesting that therapeutics designed to enhance the magnitude or duration of efferent effects on cochlear function could be beneficial in preventing OHC death. Consequently, our work provides a significant conceptual advance and points to the importance of the integrity of MOC synapses as a feedback pathway to protect inner ear function during aging. It further suggests that efferent reflex strength might be an important predictor for presbycusis–ARHL.

The α9α10 nAChR is a very peculiar member of the nAChR family. It displays a very distinct pharmacological profile that fits neither the muscarinic nor the nicotinic classification scheme of cholinergic receptors (87, 88). The present study provides a proof of principle supporting the enhancement of the MOC system as a viable approach for prevention of auditory function decline during aging. Until now, only two agents are known to potentiate α9α10 nAChR activity: ascorbic acid and ryanodine, opening the possibility of designing related compounds with improved properties for clinical use (89, 90). Therefore, finding novel positive modulators of α9α10 nAChR-mediated responses would be a significant breakthrough. Such novel therapeutics would provide new strategies for the prevention or treatment of both noise-induced and age-related hearing loss.

Materials and Methods

All experimental protocols were performed in accordance with the American Veterinary Medical Association Guidelines for the Euthanasia of Animals (June 2013), as well as Instituto de Investigaciones en Ingeniería Genética y Biología Molecular and Facultad de Medicina, Universidad de Buenos Aires Institutional Animal Care and Use Committee guidelines, and best practice procedures.

ABRs and DPOAEs were recorded to evaluate cochlear function at two different time points: 6 mo (young) and 1 y of age (aged) in mice with different levels of MOC function raised in a sound-controlled room in the animal facility.

Synapse number and other histological features were assessed in cochlear whole-mount preparations. Presynaptic ribbons were labeled with antibodies to CtBP2. Postsynaptic receptor plaques were labeled with antibodies to GluA2 subunit. Antineurofilament, heavy was used to reveal all of the unmyelinated nerve fibers. A nuclear dye, DRAQ5, was used for hair cell counting. The labeled preparations were fluorescently labeled with appropriate secondary antibodies and viewed by confocal microscopy.

Data Availability Statement. Data supporting the findings of this paper are contained within the paper and *SI Appendix*. Detailed descriptions of the procedures, ABR and DPOAE recordings and analysis, cochlear whole-mount preparation, immunofluorescent labeling, confocal imaging and quantitation, and statistics are also provided in *SI Appendix*.

ACKNOWLEDGMENTS. We thank Agustin Carpaneto-Freixas and Sebastian Iezzi for technical help. This research was supported by Agencia Nacional de Promoción Científica y Técnica (Argentina) (M.E.G.-C. and A.B.E.), the Pew Charitable Trusts (United States) (M.E.G.-C.), the National Organization for Hearing Research (United States) (M.E.G.-C.), NIH Grant R01 DC001508 (United States) (to P.A.F. and A.B.E.), Scientific Grand Prize from the Fondation Pour L´Audition (France) (to A.B.E.), Fondo Nacional de Desarrollo Científico y Tecnológico (Chile) 1161155 (to P.H.D.), Comisión Nacional de Investigación Científica y Tecnológica BASAL FB008 from Centro de Avanzado de Ingeniería Eléctrica y Electrónica (Chile) (to P.H.D.), Iniciativa Científica Milenio P09-015F from Instituto de Neurociencia Biomédica (Chile) (to P.H.D.), Proyecto REDES 150134 (Chile) (to P.H.D.), Fondos de Movilidad Institucional Universidad de O'Higgins (Chile) (G.T.), and Fundación Guillermo Puelma (Chile) (J.C.M.).

1. B. Fu *et al*., Age-related synaptic loss of the medial olivocochlear efferent innervation. *Mol. Neurodegener.* **5**, 53 (2010).
2. G. A. Gates, J. H. Mills, Presbycusis. *Lancet* **366**, 1111–1120 (2005).
3. J. A. Deal *et al*., Hearing treatment for reducing cognitive decline: Design and methods of the Aging and Cognitive Health Evaluation in Elders randomized controlled trial. *Alzheimers Dement. (N. Y.)* **4**, 499–507 (2018).
4. D. G. Loughrey, M. E. Kelly, G. A. Kelley, S. Brennan, B. A. Lawlor, Association of age-related hearing loss with cognitive function, cognitive impairment, and dementia: A systematic review and meta-analysis. *JAMA Otolaryngol. Head Neck Surg.* **144**, 115–126 (2018).
5. G. Livingston *et al*., Dementia prevention, intervention, and care. *Lancet* **390**, 2673–2734 (2017).
6. B. S. Wilson, D. L. Tucci, M. H. Merson, G. M. O'Donoghue, Global hearing health care: New findings and perspectives. *Lancet* **390**, 2503–2515 (2017).
7. M. G. Huddle *et al*., The economic impact of adult hearing loss: A systematic review. *JAMA Otolaryngol. Head Neck Surg.* **143**, 1040–1048 (2017).
8. H. M. Ren, J. Ren, W. Liu, Recognition and control of the progression of age-related hearing loss. *Rejuvenation Res.* **16**, 475–486 (2013).
9. L. F. Hughes, J. G. Turner, J. L. Parrish, D. M. Caspary, Processing of broadband stimuli across A1 layers in young and aged rats. *Hear. Res.* **264**, 79–85 (2010).
10. A. Parthasarathy, S. G. Kujawa, Synaptopathy in the aging cochlea: Characterizing early-neural deficits in auditory temporal envelope processing. *J. Neurosci.* **38**, 7108–7119 (2018).
11. D. M. Caspary, L. Ling, J. G. Turner, L. F. Hughes, Inhibitory neurotransmission, plasticity and aging in the mammalian central auditory system. *J. Exp. Biol.* **211**, 1781–1791 (2008).
12. M. C. Liberman, L. D. Liberman, S. F. Maison, Efferent feedback slows cochlear aging. *J. Neurosci.* **34**, 4599–4607 (2014).
13. M. C. Liberman, Noise-induced and age-related hearing loss: new perspectives and potential therapies. *F1000 Res.* **6**, 927 (2017).
14. S. Stamataki, H. W. Francis, M. Lehar, B. J. May, D. K. Ryugo, Synaptic alterations at inner hair cells precede spiral ganglion cell loss in aging C57BL/6J mice. *Hear. Res.* **221**, 104–118 (2006).
15. H. F. Schuknecht, R. C. Woellner, An experimental and clinical study of deafness from lesions of the cochlear nerve. *J. Laryngol. Otol.* **69**, 75–97 (1955).
16. Y. Sergeyenko, K. Lall, M. C. Liberman, S. G. Kujawa, Age-related cochlear synaptopathy: An early-onset contributor to auditory functional decline. *J. Neurosci.* **33**, 13686–13694 (2013).
17. J. A. Costalupes, Representation of tones in noise in the responses of auditory nerve fibers in cats. I. Comparison with detection thresholds. *J. Neurosci.* **5**, 3261–3269 (1985).
18. E. D. Young, P. E. Barta, Rate responses of auditory nerve fibers to tones in noise near masked threshold. *J. Acoust. Soc. Am.* **79**, 426–442 (1986).
19. C. A. Bauer, T. J. Brozoski, K. Myers, Primary afferent dendrite degeneration as a cause of tinnitus. *J. Neurosci. Res.* **85**, 1489–1498 (2007).
20. J. W. Gu, C. F. Halpin, E.-C. Nam, R. A. Levine, J. R. Melcher, Tinnitus, diminished sound-level tolerance, and elevated auditory activity in humans with clinically normal hearing sensitivity. *J. Neurophysiol.* **104**, 3361–3370 (2010).
21. A. E. Hickox, M. C. Liberman, Is noise-induced cochlear neuropathy key to the generation of hyperacusis or tinnitus? *J. Neurophysiol.* **111**, 552–564 (2014).
22. J. A. Kaltenbach, C. E. Afman, Hyperactivity in the dorsal cochlear nucleus after intense sound exposure and its resemblance to tone-evoked activity: A physiological model for tinnitus. *Hear. Res.* **140**, 165–172 (2000).
23. M. Knipper, P. Van Dijk, I. Nunes, L. Rüttiger, U. Zimmermann, Advances in the neurobiology of hearing disorders: Recent developments regarding the basis of tinnitus and hyperacusis. *Prog. Neurobiol.* **111**, 17–33 (2013).
24. R. Schaette, D. McAlpine, Tinnitus with a normal audiogram: Physiological evidence for hidden hearing loss and computational model. *J. Neurosci.* **31**, 13452–13457 (2011).
25. R. Galambos, Suppresion of auditory nerve activity by stimulation of efferent fibers to cochlea. *J. Neurophysiol.* **5**, 424–437 (1955).
26. M. L. Wiederhold, N. Y. Kiang, Effects of electric stimulation of the crossed olivocochlear bundle on single auditory-nerve fibers in the cat. *J. Acoust. Soc. Am.* **48**, 950–965 (1970).
27. J. J. Guinan, "Physiology of the medial and lateral olivocochlear systems" in *Auditory and Vestibular Efferents*, D. K. Ryugo, R. R. Fay, A. N. Popper, Eds. (Springer, 2011), pp. 39–81.
28. A. B. Elgoyhen, D. S. Johnson, J. Boulter, D. E. Vetter, S. Heinemann, Alpha 9: An acetylcholine receptor with novel pharmacological properties expressed in rat cochlear hair cells. *Cell* **79**, 705–715 (1994).
29. J. Ballestero *et al*., Short-term synaptic plasticity regulates the level of olivocochlear inhibition to auditory hair cells. *J. Neurosci.* **31**, 14763–14774 (2011).
30. E. Katz, A. B. Elgoyhen, Short-term plasticity and modulation of synaptic transmission at mammalian inhibitory cholinergic olivocochlear synapses. *Front. Syst. Neurosci.* **8**, 224 (2014).
31. M. E. Gómez-Casati, P. A. Fuchs, A. B. Elgoyhen, E. Katz, Biophysical and pharmacological characterization of nicotinic cholinergic receptors in rat cochlear inner hair cells. *J. Physiol.* **566**, 103–118 (2005).
32. J. D. Goutman, P. A. Fuchs, E. Glowatzki, Facilitating efferent inhibition of inner hair cells in the cochlea of the neonatal rat. *J. Physiol.* **566**, 49–59 (2005).
33. E. Glowatzki, P. A. Fuchs, Cholinergic synaptic inhibition of inner hair cells in the neonatal mammalian cochlea. *Science* **288**, 2366–2368 (2000).
34. P. A. Fuchs, A 'calcium capacitor' shapes cholinergic inhibition of cochlear hair cells. *J. Physiol.* **592**, 3393–3401 (2014).
35. P. H. Delano, D. Elgueda, C. M. Hamame, L. Robles, Selective attention to visual stimuli reduces cochlear sensitivity in chinchillas. *J. Neurosci.* **27**, 4146–4153 (2007).
36. G. Terreros, P. Jorratt, C. Aedo, A. B. Elgoyhen, P. H. Delano, Selective attention to visual stimuli using auditory distractors is altered in alpha-9 nicotinic receptor subunit knock-out mice. *J. Neurosci.* **36**, 7198–7209 (2016).
37. J. H. Dewson, Efferent olivocochlear bundle: Some relationships to stimulus descrimination in noise. *J. Neurophysiol.* **31**, 122–130 (1968).
38. T. Kawase, M. C. Liberman, Antimasking effects of the olivocochlear reflex. I. Enhancement of compound action potentials to masked tones. *J. Neurophysiol.* **70**, 2519–2532 (1993).
39. S. Irving, D. R. Moore, M. C. Liberman, C. J. Sumner, Olivocochlear efferent control in sound localization and experience-dependent learning. *J. Neurosci.* **31**, 2493–2501 (2011).
40. M. Handrock, J. Zeisberg, The influence of the effect system on adaptation, temporary and permanent threshold shift. *Arch. Otorhinolaryngol.* **234**, 191–195 (1982).
41. S. G. Kujawa, M. C. Liberman, Conditioning-related protection from acoustic injury: Effects of chronic deefferentation and sham surgery. *J. Neurophysiol.* **78**, 3095–3106 (1997).
42. S. F. Maison, H. Usubuchi, M. C. Liberman, Efferent feedback minimizes cochlear neuropathy from moderate noise exposure. *J. Neurosci.* **33**, 5542–5552 (2013).
43. L. E. Boero *et al*., Enhancement of the medial olivocochlear system prevents hidden hearing loss. *J. Neurosci.* **38**, 7440–7451 (2018).
44. S. F. Maison, M. C. Liberman, Predicting vulnerability to acoustic injury with a noninvasive assay of olivocochlear reflex strength. *J. Neurosci.* **20**, 4701–4707 (2000).
45. J. Taranda *et al*., A point mutation in the hair cell nicotinic cholinergic receptor prolongs cochlear inhibition and enhances noise protection. *PLoS Biol.* **7**, e18 (2009).
46. X. Zhu *et al*., Auditory efferent feedback system deficits precede age-related hearing loss: Contralateral suppression of otoacoustic emissions in mice. *J. Comp. Neurol.* **503**, 593–604 (2007).
47. R. D. Frisina, S. R. Newman, X. Zhu, Auditory efferent activation in CBA mice exceeds that of C57s for varying levels of noise. *J. Acoust. Soc. Am.* **121**, EL29–EL34 (2007).
48. G. I. Varghese, X. Zhu, R. D. Frisina, Age-related declines in distortion product otoacoustic emissions utilizing pure tone contralateral stimulation in CBA/CaJ mice. *Hear. Res.* **209**, 60–67 (2005).
49. M. L. Zettel, X. Zhu, W. E. O'Neill, R. D. Frisina, Age-related decline in Kv3.1b expression in the mouse auditory brainstem correlates with functional deficits in the medial olivocochlear efferent system. *J. Assoc. Res. Otolaryngol.* **8**, 280–293 (2007).

50. M. Jacobson, S. Kim, J. Romney, X. Zhu, R. D. Frisina, Contralateral suppression of distortion-product otoacoustic emissions declines with age: A comparison of findings in CBA mice with human listeners. *Laryngoscope* **113**, 1707–1713 (2003).
51. C. A. Shera, J. J. Guinan, Jr, Evoked otoacoustic emissions arise by two fundamentally different mechanisms: A taxonomy for mammalian OAEs. *J. Acoust. Soc. Am.* **105**, 782–798 (1999).
52. L. Robles, M. A. Ruggero, Mechanics of the mammalian cochlea. *Physiol. Rev.* **81**, 1305–1352 (2001).
53. D. Robertson, M. Gummer, Physiological and morphological characterization of efferent neurones in the guinea pig cochlea. *Hear. Res.* **20**, 63–77 (1985).
54. M. C. Liberman, Physiology of cochlear efferent and afferent neurons: Direct comparisons in the same animal. *Hear. Res.* **34**, 179–191 (1988).
55. J. S. Buchwald, C. M. Huang, Far-field acoustic response: Origins in the cat. *Science* **189**, 382–384 (1975).
56. S. G. Kujawa, M. C. Liberman, Adding insult to injury: Cochlear nerve degeneration after "temporary" noise-induced hearing loss. *J. Neurosci.* **29**, 14077–14085 (2009).
57. D. Khimich *et al*., Hair cell synaptic ribbons are essential for synchronous auditory signalling. *Nature* **434**, 889–894 (2005).
58. A. Matsubara, J. H. Laake, S. Davanger, S. Usami, O. P. Ottersen, Organization of AMPA receptor subunits at a glutamate synapse: A quantitative immunogold analysis of hair cell synapses in the rat organ of Corti. *J. Neurosci.* **16**, 4457–4467 (1996).
59. L. D. Liberman, H. Wang, M. C. Liberman, Opposing gradients of ribbon size and AMPA receptor expression underlie sensitivity differences among cochlear-nerve/hair-cell synapses. *J. Neurosci.* **31**, 801–808 (2011).
60. F. Gilels, S. T. Paquette, J. Zhang, I. Rahman, P. M. White, Mutation of Foxo3 causes adult onset auditory neuropathy and alters cochlear synapse architecture in mice. *J. Neurosci.* **33**, 18409–18424 (2013).
61. S. T. Paquette, F. Gilels, P. M. White, Noise exposure modulates cochlear inner hair cell ribbon volumes, correlating with changes in auditory measures in the FVB/nJ mouse. *Sci. Rep.* **6**, 25056 (2016).
62. K. A. Fernandez, P. W. Jeffers, K. Lall, M. C. Liberman, S. G. Kujawa, Aging after noise exposure: Acceleration of cochlear synaptopathy in "recovered" ears. *J. Neurosci.* **35**, 7509–7520 (2015).
63. M. C. Liberman, Efferent synapses in the inner hair cell area of the cat cochlea: An electron microscopic study of serial sections. *Hear. Res.* **3**, 189–204 (1980).
64. S. G. Kujawa, M. C. Liberman, Synaptopathy in the noise-exposed and aging cochlea: Primary neural degeneration in acquired sensorineural hearing loss. *Hear. Res.* **330**, 191–199 (2015).
65. J. R. Dubno, D. D. Dirks, D. E. Morgan, Effects of age and mild hearing loss on speech recognition in noise. *J. Acoust. Soc. Am.* **76**, 87–96 (1984).
66. S. Gordon-Salant, P. J. Fitzgibbons, Temporal factors and speech recognition performance in young and elderly listeners. *J. Speech Hear. Res.* **36**, 1276–1285 (1993).
67. K. B. Snell, D. R. Frisina, Relationships among age-related differences in gap detection and word recognition. *J. Acoust. Soc. Am.* **107**, 1615–1626 (2000).
68. J. P. Walton, Timing is everything: Temporal processing deficits in the aged auditory brainstem. *Hear. Res.* **264**, 63–69 (2010).
69. D. Ruggles, H. Bharadwaj, B. G. Shinn-Cunningham, Why middle-aged listeners have trouble hearing in everyday settings. *Curr. Biol.* **22**, 1417–1422 (2012).
70. A. C. Furman, S. G. Kujawa, M. C. Liberman, Noise-induced cochlear neuropathy is selective for fibers with low spontaneous rates. *J. Neurophysiol.* **110**, 577–586 (2013).
71. R. A. Schmiedt, J. H. Mills, F. A. Boettcher, Age-related loss of activity of auditory-nerve fibers. *J. Neurophysiol.* **76**, 2799–2803 (1996).
72. M. C. Liberman, Single-neuron labeling in the cat auditory nerve. *Science* **216**, 1239–1241 (1982).
73. R. A. Schmiedt, B. A. Schulte, "Physiologic and histopathologic changes in quiet- and noise-aged gerbil cochleas" in *Noise Induced Hearing Loss*, A. L. Dancer, D. Henderson, R. J. Salvi, R. P. Hamernik, Eds. (Mosby, 1992), pp. 246–258.
74. J. J. Guinan, P. Dallos, A. N. Popper, R. R. Fay, "Efferent physiology" in *The Cochlea*, P. Dallos, A. N. Popper, R. R. Fay, Eds. (Springer, 1996), pp. 435–502.
75. D. F. Dolan, A. L. Nuttall, Masked cochlear whole-nerve response intensity functions altered by electrical stimulation of the crossed olivocochlear bundle. *J. Acoust. Soc. Am.* **83**, 1081–1086 (1988).
76. R. L. Winslow, M. B. Sachs, Single-tone intensity discrimination based on auditory-nerve rate responses in backgrounds of quiet, noise, and with stimulation of the crossed olivocochlear bundle. *Hear. Res.* **35**, 165–189 (1988).
77. M. C. Liberman, The olivocochlear efferent bundle and susceptibility of the inner ear to acoustic injury. *J. Neurophysiol.* **65**, 123–132 (1991).
78. S. F. Maison, A. E. Luebke, M. C. Liberman, J. Zuo, Efferent protection from acoustic injury is mediated via alpha9 nicotinic acetylcholine receptors on outer hair cells. *J. Neurosci.* **22**, 10838–10846 (2002).
79. S. F. Maison, J. C. Adams, M. C. Liberman, Olivocochlear innervation in the mouse: Immunocytochemical maps, crossed versus uncrossed contributions, and transmitter colocalization. *J. Comp. Neurol.* **455**, 406–416 (2003).
80. V. P. Spongr, D. G. Flood, R. D. Frisina, R. J. Salvi, Quantitative measures of hair cell loss in CBA and C57BL/6 mice throughout their life spans. *J. Acoust. Soc. Am.* **101**, 3546–3553 (1997).
81. K. K. Ohlemiller, A. R. Dahl, P. M. Gagnon, Divergent aging characteristics in CBA/J and CBA/CaJ mouse cochleae. *J. Assoc. Res. Otolaryngol.* **11**, 605–623 (2010).
82. J. J. Guinan, Jr, Olivocochlear efferents: Anatomy, physiology, function, and the measurement of efferent effects in humans. *Ear Hear.* **27**, 589–607 (2006).
83. M. C. Liberman, W. Y. Gao, Chronic cochlear de-efferentation and susceptibility to permanent acoustic injury. *Hear. Res.* **90**, 158–168 (1995).
84. S. F. Maison, R. B. Emeson, J. C. Adams, A. E. Luebke, M. C. Liberman, Loss of alpha CGRP reduces sound-evoked activity in the cochlear nerve. *J. Neurophysiol.* **90**, 2941–2949 (2003).
85. S. G. Kujawa, M. C. Liberman, Translating animal models to human therapeutics in noise-induced and age-related hearing loss. *Hear. Res.* **377**, 44–52 (2019).
86. L. D. Liberman, M. C. Liberman, Cochlear efferent innervation is sparse in humans and decreases with age. *J. Neurosci.* **39**, 9560–9569 (2019).
87. M. Verbitsky, C. V. Rothlin, E. Katz, A. B. Elgoyhen, Mixed nicotinic-muscarinic properties of the alpha9 nicotinic cholinergic receptor. *Neuropharmacology* **39**, 2515–2524 (2000).
88. A. B. Elgoyhen *et al*., alpha10: A determinant of nicotinic cholinergic receptor function in mammalian vestibular and cochlear mechanosensory hair cells. *Proc. Natl. Acad. Sci. U.S.A.* **98**, 3501–3506 (2001).
89. J. Zorrilla de San Martín, J. Ballestero, E. Katz, A. B. Elgoyhen, P. A. Fuchs, Ryanodine is a positive modulator of acetylcholine receptor gating in cochlear hair cells. *J. Assoc. Res. Otolaryngol.* **8**, 474–483 (2007).
90. J. C. Boffi *et al*., Positive modulation of the $\alpha 9\alpha 10$ nicotinic cholinergic receptor by ascorbic acid. *Br. J. Pharmacol.* **168**, 954–965 (2013).